


Productivity of a Continuous Mining System for Block Caving Mines

L. F. Orellana^{1,2}  · R. Castro^{1,2} · A. Hekmat^{1,2} · E. Arancibia³

Received: 14 March 2016 / Accepted: 28 September 2016 / Published online: 12 October 2016
© Springer-Verlag Wien 2016

Keywords Underground mining · Block caving mines · Continuous mining system · Physical modeling · Intermittent flow

x_{ss} Steady-state production rate
 α Conversion factor from grams to tons
 β Conversion factor from seconds to minutes

List of symbols

λ_l	Geometric scale factor
λ_t	Time scale factor
λ_v	Velocity scale factor
\bar{x}_j	Productivity of the material j in grams per cycle (laboratory data)
\bar{x}'_j	Scaled productivity (laboratory to mine scale) in t/cycle
\bar{x}''_j	Scaled productivity (laboratory to mine scale) in m ³ /cycle
ρ_{aj}	Apparent density of the material j
CAE_{jn}	Cumulative average extraction of the material j calculated for the total number of cycles n
V_{ij}	Scaled volume of the material j in the cycle i
x_{ij}^{lab}	The amount of mass extracted from the material j in grams per cycle in the cycle i
T_{nj}	Cumulative time of each material j calculated for the total number of cycles n
t_{ij}	The time to complete the full loading–discharging cycle i of the material j
$t_{50\%}$	The time at which 50 % of the steady-state production rate x_{ss} is reached

1 Introduction

Block caving mining is one of the most cost-effective underground mining methods. The method has particular relevance in the Chilean mining industry, where approximately 40 % of the Chilean national copper production comes from block caving mines (El Teniente, Andina, and El Salvador, and in the near future, Chuquicamata). As a consequence of the industry needing to increase productivity, Caterpillar (CAT) and Codelco (the National Copper Corporation of Chile) developed the Rock Flow Continuous Mining System (CAT 2015).

The new system aims to raise productivity from 0.4 to 1 t/day m², by using continuous haulage technology instead of the conventional use of LHD—Load, Haul, Dump machine—(Encina et al. 2008; CAT 2015). The first prototype trial took place in 2005 at the El Salvador mine, Chile, reaching a mean production rate of 200 t/h (Encina et al. 2008; Orellana 2012).

The RFCMS chains a group of feeders, a heavy-weight conveyor, and a primary crusher. Early crushing of the mineral was introduced to avoid grizzlies on ore passes and to allow proper operation on conveyors belts. Each feeder extracts ore from the draw points, which feeds the conveyor equipped with a primary crusher. Concerning a large cave operation (i.e., hundreds of draw points operating at the same time), the RFMCS operates through production modules working in coordination, to secure the production capacity of the mine.

✉ L. F. Orellana
luisfelipe.orellana@ing.uchile.cl

¹ Advanced Mining Technology Center, Universidad de Chile, Santiago, Chile

² Department of Mining Engineering, Universidad de Chile, Santiago, Chile

³ Codelco, Santiago, Chile

Through physical modeling (Kvapil 1965; Laubscher 1994; Power 2004; Castro et al. 2007; Trueman et al. 2008; Alejano et al. 2011; Castro et al. 2014), the current project examines the production capacity of the dozer feeder system for different material types.

The objective of this technical procedure is to explore the suitability of different rock-type materials for physical modeling and to derive adjustment factors to upscale the productivity (t/h) of the system. The comparison between laboratory production rates and real field data showed good agreement for some of the materials under evaluation. In this note, we introduced a new model of productivity and steady-state production rates for the current material handling system.

2 Experimental Setup

Six experiments were carried out using materials with different rock properties. An axisymmetric 2D physical model was built aiming to mimic the continuous rock extraction system in one draw point. It represented a 50-m fragmented column of ore mineral. Intermittent flow under low stress conditions was chosen as the most representative cave mining environment (Castro et al. 2014). Materials with various shapes and strength characteristics, yet same particle size distributions, were considered, and productivity and velocity of the dozer feeder were measured. This experimental setup resembles the mobilized zone, where the ore is already fragmented. The current model does not intend to model the caving process on an intact rock. However, it does intend to represent the production process of the RFCMS.

The geometrical scale was defined as $\lambda_l = \frac{1}{50}$. This satisfies the construction of all parts of the model and ensures representation of the phenomena. According to scaling laws, time and velocity scales are equal to the square of the geometrical scale, $\lambda_t = \lambda_v = \lambda_l^{1/2}$. The weight scale factor is λ_f^3 . The total height of the draw column in the physical model is 1 m. The main dimensions of the scaled dozer (Fig. 1) and the physical model (Fig. 2) are presented in Table 1.

The dozer or feeder system is installed below the material column inside the draw point. A pneumatic system has been designed to facilitate the two movements of the dozer: inside and outside of the ore column (Fig. 3). The productivity and pushing pressure were measured in terms of mass per cycle and bar, respectively. Manometers allow for the measurement of the minimal pressure required by the system to ensure full movement.

The procedure consisted of applying a constant pressure to the dozer during the cycle until a quantity of material was extracted from the draw point. The cycle begins when the dozer remains stationary below the material column (Fig. 3a). The dozer then pushes the fragments into the empty space (Fig. 3b), allowing them to be weighed by an electronic load cell. Finally, the dozer returns to its initial position (Fig. 3c) and is ready to start a new cycle. The experiment is completed once the first colored marker, which originated from the top of the model at the beginning of the test, is recovered.

2.1 Material Characterization

For each type of material, classes of fragments were sieved and mixed to achieve the same size distribution for all rounds. The particle size distribution used in the experiments replicates the size distribution encountered at the draw points in the El Salvador in situ test. Fragments with equivalent diameter below 0.64 cm were discarded for operational reasons, but they were later considered for productivity calculations. The physical model design followed a ratio of draw point/width to particle size (d_w/d_{50}) equal to 5.2, ensuring an intermittent flow environment (Castro et al. 2014).

Crushed copper ore, gravel, mortar, brick, gypsum, and charcoal were used in the experiments. Copper ore rocks were obtained from the El Salvador mine. Gravel, brick, and charcoal were acquired from a construction materials store. Mortar and gypsum fragments were prepared in the laboratory. The properties measured are presented in Table 2.

The strength index of each material was measured by using the ASTM D5731-08 point load test procedure. The materials were classified based on their particle shape



Fig. 1 Dozer feeder system at reduced scale. **a** Isometric view at the draw point, **b** plan view, and **c** lateral view

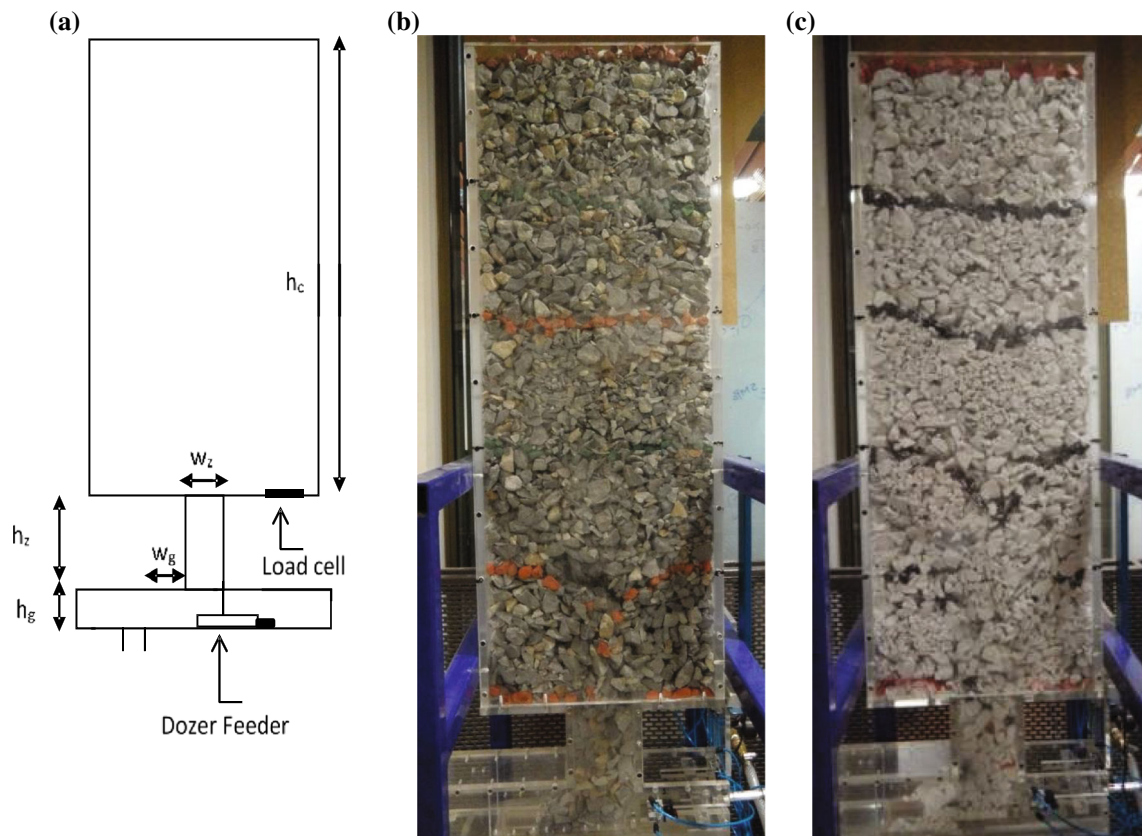


Fig. 2 Physical model for studying the rock continuous system **a** schematic view of the model (not at scale), **b** model filled with gypsum fragments, and **c** model filled with mineral fragments during extraction of material

Table 1 Physical model dimensions

Item	Symbol	Scaled model		Actual (mine) size	
		Unit	Value	Unit	Value
Fragmented column height	h_c	mm	1000	m	50
Draw-bell angle	B	°	90	°	90
Draw-bell height	h_z	mm	150	m	7.5
Draw-bell width	w_z	mm	94	m	4.7
Gallery area	A	mm ²	6400	m ²	16
Gallery height	h_g	mm	80	m	4
Distance to road	w_g	mm	62	m	3.1
Dozer length		mm	11	m	5.5
Dozer width		mm	4	m	2

(Santamarina and Cho 2004). Thirty d_{50} size fragments of each material were analyzed. As a result, copper ore and gravel were classified as angular and sub-round, respectively, while the other materials were classified as sub-angular.

Specific density was measured in the laboratory using water pycnometry at room temperature. Apparent (bulk) density was calculated using the ratio between mass and given volume. Both the weight of a representative sample

of the material (obtained using a rotary sampler) and the dimensions of the recipient were known.

3 Results

Six trials were carried out during this research as presented in Table 3. The variables measured during the experiments included: production per cycle (g/cycle) and cycle time (s).

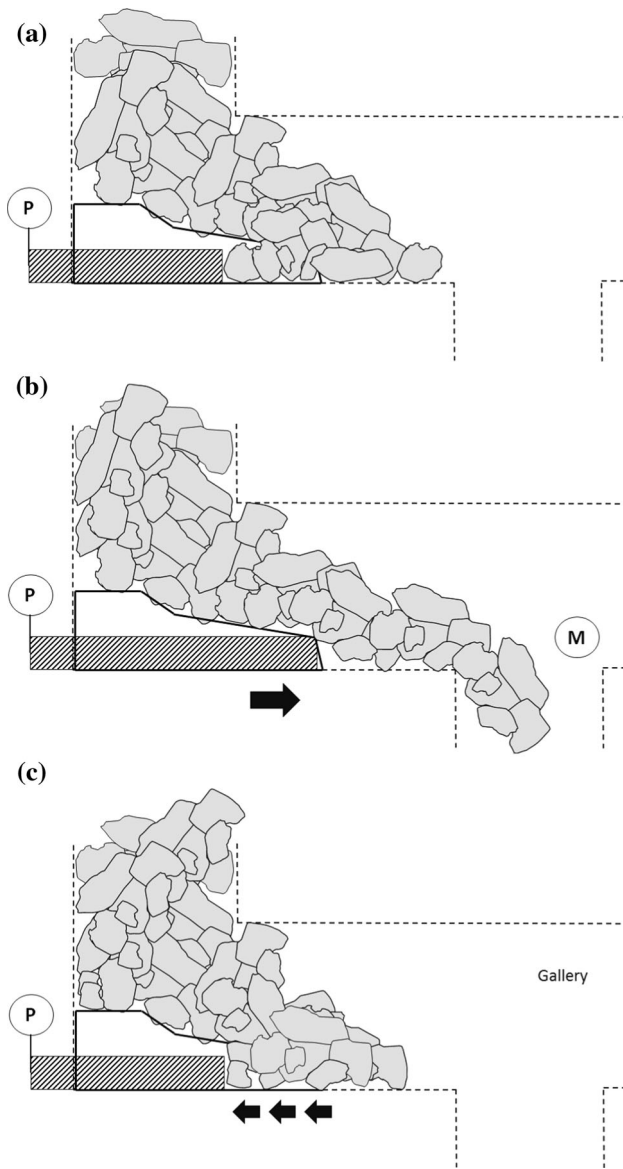


Fig. 3 Schematic representation of a production cycle **a** dozer feeder remains stationary, **b** dozer goes forward pushing fragments, and **c** after the equipment moves along the gallery, it returns to its initial position

4 Discussion

Particle shape can be the reason for the highest observed value of productivity of the gravel material as it has been pointed out that rounded particles flow easily (Santamarina and Cho 2004). Table 4 presents the laboratory values scaled up to data from the El Salvador test.

In Table 4, \bar{x}_j is equal to the laboratory production average of the material j in grams per cycle, ρ_{aj} is the apparent density (Table 2) of the material j , $\alpha = 10^6$ is the unity conversion value from grams to tons, and λ_j^3 represents the scaled factor for weight. In order to compare the laboratory results with the prototype, we defined the cumulative average extraction (CAE) of the material j as:

$$CAE_{jn} = \sum_{i=1}^n \frac{V_{ij}}{n} \tag{1}$$

In Eq. 1, $i \dots n$ represents a cycle, where n is the last one, V_{ij} corresponds to the scaled volume of the material j and was calculated from the production rate measured in the laboratory:

$$V_{ij} \left(\frac{\text{m}^3}{\text{cycle}} \right) = \frac{x_{ij}^{\text{lab}}}{\alpha \cdot \rho_{aj} \cdot \lambda_j^3} \tag{2}$$

where x_{ij}^{lab} is the amount of mass extracted from the material j in grams per cycle in the cycle i . The cumulative time T_{nj} of each material j was defined as the addition of all cycle times:

$$T_{nj}(\text{min}) = \left(\frac{1}{\beta \cdot \lambda_j^2} \right) \cdot \sum_{i=1}^n t_{ij}(\text{s}) \tag{3}$$

The value t_{ij} corresponds to the time to complete the full loading–discharging cycle i of the material j , $\beta = \frac{1}{60}$ is the unity conversion value from seconds to minutes, and λ_j^2 represents the scaled factor for time. The time T_{nj} also represents the duration needed to finish an experiment.

Table 2 Material properties

Material property	Unit	Copper ore	Gravel	Mortar	Brick	Gypsum	Charcoal
Particle size							
d_{80}	cm	2.44					
d_{50}	cm	1.81					
Uniformity index (d_{60}/d_{10})	–	2.17					
Particle shape							
Sphericity		0.64	0.65	0.57	0.57	0.55	0.51
Roundness		0.11	0.44	0.27	0.25	0.24	0.23
Regularity		0.37	0.54	0.42	0.41	0.39	0.37
Specific density	g/cm^3	2.71	2.69	2.59	2.68	2.84	0.83
Apparent density	g/cm^3	1.57	1.61	0.92	1.02	0.97	0.42

Table 3 Laboratory results

	Productivity (g/cycle) [mean ± variance]	Cycle time (s) [mean ± variance]	Dozer velocity (mm/s) [mean ± variance]
Copper ore	28.6 ± 35.5	11.2 ± 1.9	2.4 ± 1.0
Gravel	31.5 ± 36.3	10.9 ± 1.9	2.8 ± 1.6
Mortar	10.3 ± 15.7	11.0 ± 1.7	2.7 ± 0.5
Brick	15.4 ± 18.0	11.1 ± 1.6	2.7 ± 0.6
Gypsum	6.2 ± 9.5	11.0 ± 1.5	2.7 ± 1.1
Charcoal	3.0 ± 4.0	11.0 ± 1.2	2.7 ± 0.5

Table 4 Scaled values of laboratory results

Material	Laboratory productivity (g/cycle) $\bar{x}_j \pm \sigma_j$		Scaled productivity (mine) (t/cycle) $\bar{x}'_j = \frac{(\bar{x}_j \pm \sigma_j)}{\alpha \cdot \lambda_i^3}$		Scaled productivity (mine) (m ³ /cycle) $\bar{x}''_j = \frac{(\bar{x}_j \pm \sigma_j)}{\alpha \cdot \rho_{aj} \cdot \lambda_i^3}$	
	Mean	Variance	Mean	Variance	Mean	Variance
Copper ore	28.6	35.5	3.6	4.4	2.3	2.8
Gravel	31.5	36.3	4.0	4.5	2.4	2.8
Mortar	10.3	15.7	1.3	2.0	1.4	2.1
Brick	15.4	18.0	1.9	2.3	1.9	2.2
Gypsum	6.2	9.5	0.8	1.2	0.8	1.2
Charcoal	3.0	5.0	0.4	0.6	0.9	1.5

The data are fitted by the equation $y = \frac{x_{ss} \cdot t}{t_{50\%} + t}$. The parameters for each material are presented in Table 5. The parameter $t_{50\%}$ represents the time at which 50 % of the steady-state production rate x_{ss} is reached. Figure 4 shows the evolution of parameter CAE_{nj} with respect to T_{nj} .

The data from Fig. 4 show that the copper ore and gravel showed similar behaviors. The rest of the materials are far below the productivity average and the steady-state values as compared to the copper ore results. As was previously indicated, the measured in situ test productivity was 200 t/h. From the laboratory test, 45 cycles/h (scaled time by $\lambda_i^{1/2}$) on average were recorded. On combining both results, a production rate of 2.8 m³/cycle was obtained for the El Salvador test, using an apparent density of 1.57 t/m³ (Table 2). The two main reasons for the observed differences are as follows:

1. *Size distribution* The size distribution used in the experiments has a lower limit of 0.635 cm. This fraction represents 8.23 % of the particle size distribution observed at the mine. This constraint is necessary for the smooth operation of the physical model. Fragment sizes below 0.635 cm caused a large number of operational interruptions in the physical model unrelated to the mine conditions. Laubscher (1994) indicated that on average, for a very coarse material, approximately 22 % of the material makes up less than 0.12 m³. Thus, a correction factor of 1.08–1.25 can be applied to account for material less than 0.12 m³ in the physical model.
2. *Zero production cycles* During the physical modeling, null productive cycles were observed, sometimes accompanied by hang-ups. For this study, those cycles were recorded and considered part of the production system. Encina et al. (2008) have not provided any additional information concerning this issue. Notably, during the extraction of copper ore fragments, 18.2 % of the cycles were recorded as “zero production cycles.” A correction factor of 1.18 (Table 6) was applied to account for the zero production cycles in the physical model.

In conclusion, the average \bar{x}'_j and the steady-state x_{ss} productivity rate values should be corrected by applying a factor of $cf_1 = 1.15$ and $cf_2(\text{copper ore}) = 1.18$ (if zero production cycles are not considered).

Table 5 Parameters model

Material/parameter	$x_{ss} \left(\frac{m^3}{\text{cycle}} \right)$	$t_{50\%}$ (min)
Copper ore	2.5	37.7
Gravel	2.7	66.7
Mortar	1.4	6.3
Brick	2.0	24.8
Gypsum	0.8	4.4
Charcoal	0.8	18.2

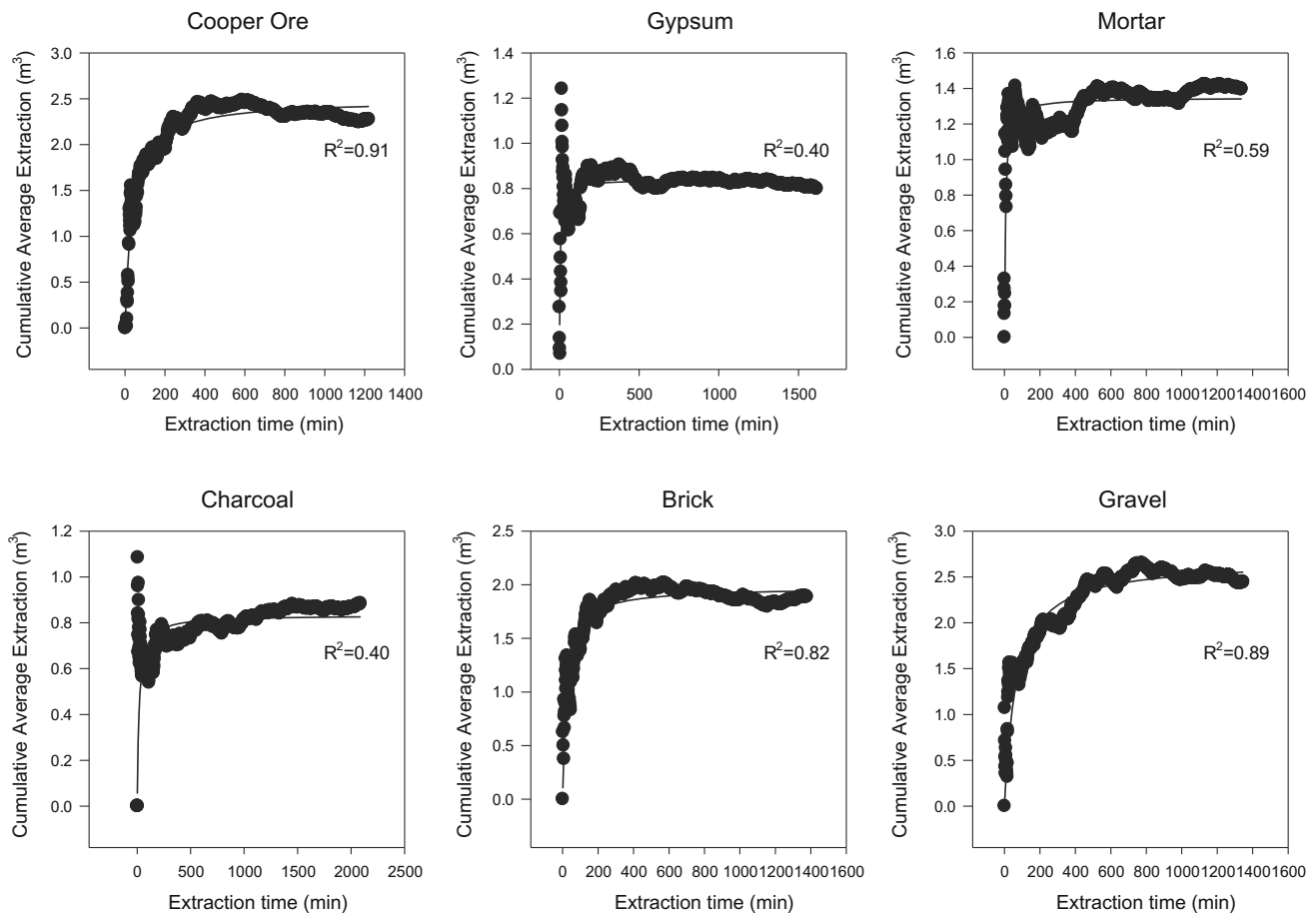


Fig. 4 Cumulative average extraction plotted against the cumulative time for each material

Table 6 Correction factors and corrected productivity rates indexes

Correction factor $cf_1 = 1.15$		$\bar{x}'_j \left(\frac{m^3}{\text{cycle}} \right)$	$x_{ss} \left(\frac{m^3}{\text{cycle}} \right)$
Material	Correction factor cf_2	$cf_1 \cdot cf_2 \cdot \bar{x}'_j$	$cf_1 \cdot cf_2 \cdot x_{ss}$
Copper ore	1.18	3.1	3.4
Gravel	1.15	3.2	3.5
Mortar	1.10	1.8	1.71
Brick	1.18	2.6	2.7
Gypsum	1.28	1.2	1.2
Charcoal	1.36	1.4	1.3

Table 6 shows the copper ore (3.1 m³/cycle), gravel (3.2 m³/cycle), and brick (2.6 m³/cycle) productivity rates as the closest values matching the productivity rates measured at the mine (2.8 m³/cycle). Moreover, the steady-state productivity indicates that a higher production can be expected at the mine. Particle shape can be argued as the reason for the higher productivity of the gravel material, as rounded particles tend to flow more easily.

5 Conclusions

The continuous mining system for block caving mines was modeled under laboratory-scaled conditions. Indeed, there is a good agreement between the El Salvador mine test results and the scaled values in terms of productivity, where copper ore fragments, gravel, and brick were used. A full characterization of average and steady-state production is provided. Moreover, a model of productivity is presented in terms of extraction time and average productivity. This model can prove helpful for engineers for future modeling of the continuous extraction rock system for caving mines. For instance, in a production module of six feeders, the productivity rates encountered can help to estimate the production capacity of the module under certain conditions of operation. If we consider two shifts per day of 8 operational hours, one feeder will extract around 2450 m³/day. This rate, of course, will depend on the shift arrangement, maintenance, mine sequencing, and others operational factors of the cave mine.

Even though there is a large difference between the productivity of charcoal, gypsum, and mortar materials (at

a production rate of 200 t/h), the ability to relate productivity rates to the use of the material is a key finding. The application of adjustment factors for engineering design purposes has proved to be very useful.

Acknowledgments The authors would like to acknowledge the financial support of the Chilean government through the project Conicyt FB0809. We acknowledge the support and permission of Codelco to publish this article.

References

- Alejano LR, Ferrero AM, Ramírez-Oyanguren P, Álvarez Fernández MI (2011) Comparison of limit-equilibrium, numerical and physical models of wall slope stability. *Int J Rock Mech Min Sci* 48:16–26. doi:[10.1016/j.ijrmms.2010.06.013](https://doi.org/10.1016/j.ijrmms.2010.06.013)
- Castro RL, Trueman R, Halim A (2007) A study of isolated draw zones in block caving mines by means of a large 3D physical model. *Int J Rock Mech Min Sci* 44:860–870. doi:[10.1016/j.ijrmms.2007.01.001](https://doi.org/10.1016/j.ijrmms.2007.01.001)
- Castro RL, Fuenzalida MA, Lund F (2014) Experimental study of gravity flow under confined conditions. *Int J Rock Mech Min Sci* 67:164–169. doi:[10.1016/j.ijrmms.2014.01.013](https://doi.org/10.1016/j.ijrmms.2014.01.013)
- CAT (2015) CAT (R) rock flow system. http://www.cat.com/en_US/products/new/equipment/underground-hard-rock/rock-flow-system/18513467.html
- Encina V, Baez F, Geister F, Steinberg J (2008) Mechanized continuous drawing system: a technical answer to increase production capacity for large block caving mines. In: Schunnesson H, Nordlund E (eds) *MassMin 2008: proceedings of the 5th international conference and exhibition on mass mining*. Luleå, Sweden, pp 553–562
- Kvapil R (1965) Gravity flow of granular materials in Hoppers and bins in mines—II. Coarse material. *Int J Rock Mech Min Sci Geomech Abstr* 2:277–292. doi:[10.1016/0148-9062\(65\)90029-X](https://doi.org/10.1016/0148-9062(65)90029-X)
- Laubscher D (1994) Cave mining—the state of the art. *J South Afr Inst Min Metall* 94(10):279–293
- Orellana LF (2012) Study the design variables of continuous mining system based on laboratory experimentation. Department of Mining Engineering. Master Thesis, University of Chile, Santiago, Chile, p 214
- Power G (2004) Modelling granular flow in caving mines: large scale physical modeling and full scale experiments. PhD Thesis, The University of Queensland, Brisbane, Australia
- Santamarina J, Cho G (2004) Soil behaviour: the role of particle shape. *Adv Geotech Eng Proc Skempton Conf* 1–14. http://pmrl.ce.gatech.edu/tools/santamarina_cho_2004.pdf
- Trueman R, Castro RL, Halim A (2008) Study of multiple draw-zone interaction in block caving mines by means of a large 3D physical model. *Int J Rock Mech Min Sci* 45:1044–1051. doi:[10.1016/j.ijrmms.2007.11.002](https://doi.org/10.1016/j.ijrmms.2007.11.002)